Chapter 1
Introduction to Luminescence Signals and Models

1.1 Thermally and Optically Stimulated Luminescence Phenomena

In this introductory chapter we describe several types of thermally and optically luminescence signals, which form the basis of luminescence dosimetry and luminescence dating.

The interaction of ionizing radiation with both natural and artificial inorganic materials makes these materials suitable to act as radiation detectors. An important family of radiation detectors, called passive detectors, is based on the existence of localized energy levels within the forbidden energy band. These energy levels are created by the presence of imperfections and impurities in the crystal lattice and by the irradiation of these materials in nature or in the laboratory.

In the framework of the phenomenological energy band model of solids, the irradiation process creates electrons in the conduction band and holes in the valence band. The electrons from the conduction band are trapped in electron traps, and the holes are trapped in hole traps (which can also act as luminescence centers) within the forbidden band.

After irradiation, the system is in an excited state, and the lifetime of these excited states in nature varies widely from microseconds to billions of years. When the material is thermally or optically stimulated in the laboratory, the trapped electrons are released and may eventually recombine with holes at luminescence centers, thus causing the emission of light from the sample. The property making the material a dosimeter is the functional relationship between the number of electrons trapped in the material and the irradiation dose.

Various stimulation methods are commonly used in the laboratory to liberate the trapped electrons, and these methods generate different types of stimulated luminescence (SL) signals. In terms of the time scales involved in luminescence processes, one can distinguish two broad types of experiments. In the first category one studies phenomena such as thermoluminescence (TL) or optically stimulated luminescence (OSL) that take place in time scales of seconds. A general description

© The Author(s), under exclusive license to Springer Nature Switzerland AG 2021

V. Pagonis, *Luminescence*, Use R!, https://doi.org/10.1007/978-3-030-67311-6_1

of TL signals and associated delocalized and localized transition models is given in Sect. 1.2, followed by a discussion of isothermal TL (ITL) signals in Sect. 1.3. An overview of OSL signals measured with visible and infrared light is presented in Sect. 1.4.

In the second broad category of experiments one studies time-resolved (TR) phenomena, where researchers use short light pulses to separate the stimulation and emission of luminescence in time. TR experiments usually involve much shorter time scales than TL/OSL, typically of the order of milliseconds or microseconds. An overview of TR signals is given in Sect. 1.5 of this chapter. Section 1.6 presents a brief description of electron spin resonance (ESR) signals and optical absorption (OA) signals, and their connection and importance in luminescence dosimetry. Finally, this chapter concludes in Sect. 1.7 with a brief discussion of what types of information researchers typically extract from the experimental data described in this chapter.

For a comprehensive review of the phenomena described in this book, the readers are directed to several available excellent textbooks and review articles on luminescence dosimetry and its applications (Chen and Pagonis [38], Yukihara and McKeever [195], Pagonis et al. [137], Böetter-Jensen et al. [19], Chen and McKeever [37]).

1.2 Overview of Thermoluminescence (TL) Signals and Models

When the stimulation of the sample in the laboratory is thermal, the phenomenon is called *thermoluminescence* (TL) or *thermally stimulated luminescence* (TSL). Commonly used experimental heating functions during a TL experiment are linear, hyperbolic, and exponential heating functions.

During a TL experiment, one records the light intensity as a function of temperature, and the total signal is termed a *TL glow curve*. An example of a TL glow curve measured with a constant heating rate is shown in Fig. 1.1a, for a synthetic quartz sample (Kitis et al. [76]). In Fig. 1.1b, the TL signal from the same sample is plotted as a function of the irradiation dose; this type of graph is usually referred to as the *TL dose response curve*.

The analysis of complex TL glow curves like the one shown in Fig. 1.1a is known as the deconvolution of the TL glow curve and is discussed in detail in Chap. 2. The analysis of dose response data similar to Fig. 1.1b is covered in detail in Chap. 4.

An example of TL glow curves measured after irradiation with different doses is given in Fig. 1.2, for the dosimetric material MgB_4O_7:Dy,Na or MBO (Pagonis et al. [124]). This data shows that as the irradiation dose is increased, the height of the TL peak increases proportionally to the irradiation doses of (1,3,4,6) Gy. At the same time, the shape of the TL peak remains unchanged. This is shown in Fig. 1.2b, where the TL peaks were normalized by multiplying each one with an appropriate scaling

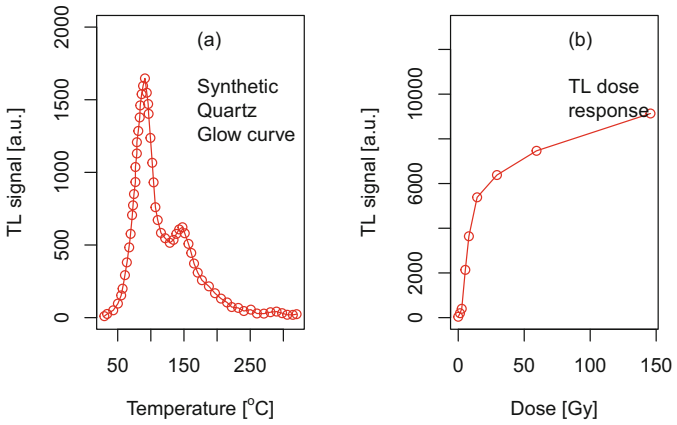

Fig. 1.1 (**a**) Example of a TL glow curve for synthetic quartz, after irradiation with a beta dose of 2 Gy. (**b**) The TL dose response of this quartz sample, obtained by plotting the maximum intensity of the TL signal as a function of the irradiation dose. For more details, see Kitis et al. [76]

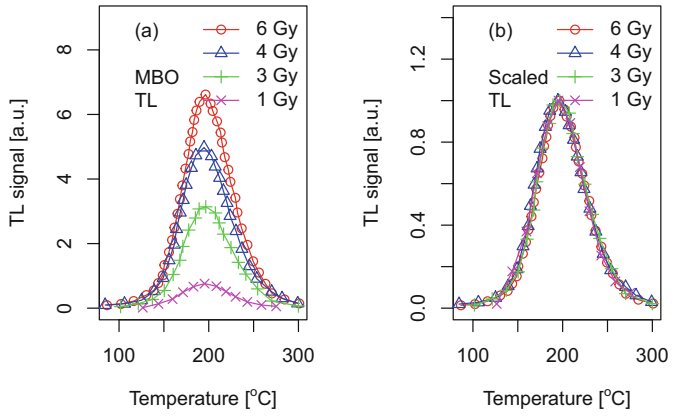

Fig. 1.2 (**a**) Example of a series of TL glow curves for sample MBO, at different beta doses. (**b**) The data in (**a**) is normalized to the maximum TL height. For more details, see Pagonis et al. [124]

factor, so that their maximum heights are 1. This type of behavior as a function of irradiation dose, in which the shape of the TL peak and the temperature of maximum height remain unchanged, is described as *first order kinetics*. The general theory of first order kinetics (FOK) and of other types of kinetics is discussed in detail in Chaps. 2 and 3.

The shape of the TL glow curves, the number of peaks, and their temperature are of particular interest to researchers developing new dosimetric materials. Figure 1.3 shows a comparison of the TL glow curves for the dosimetric materials MgB_4O_7:Dy,Na (MBO) and LiB_4O_7:Cu,In (LBO) (Kitis et al. [81]). The TL glow curves were obtained by irradiating the samples with the same dose and

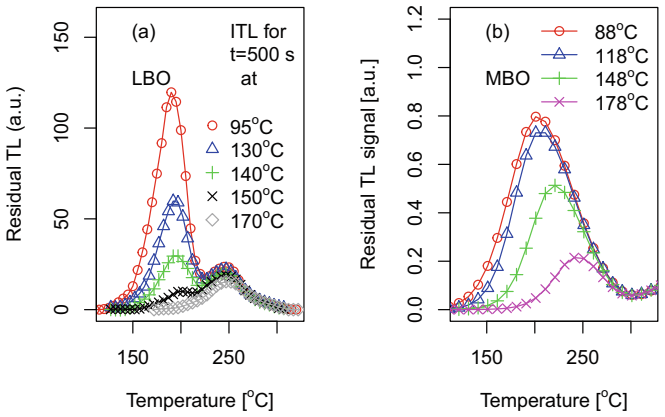

Fig. 1.3 (**a**) Example of a series of TL glow curves for sample LBO, after irradiation and heating up to the temperatures indicated in the legends. (**b**) A very similar series of TL glow curves for sample MBO. The different behaviors of these two samples indicate that different luminescence mechanisms are involved in each case. For more details, see Kitis et al. [81]

subsequently heating the sample up to the temperatures indicated in the legends of Fig. 1.3a, b. Note that the shapes and widths of the main dosimetric peaks around 200 °C in these two materials are very different. The overall shape of the TL peak in LBO is asymmetric, while the TL peak in MBO is very nearly symmetric.

In addition to the differences in their widths, the TL peaks behave very differently in Fig. 1.3a, b. The temperature of the maximum intensity ($T_{\max}$) in the series of TL glow curves in Fig. 1.3a does not shift significantly, while the corresponding $T_{\max}$ changes continuously in the series of TL glow curves in Fig. 1.3b.

In the above example for materials LBO and MBO, the different behaviors of the TL glow curves point to the possibility that a different luminescence mechanism is involved in these materials.

In fact, the luminescence mechanism for LBO can be explained using a *delocalized transitions model* that involves the conduction and valence bands, while the mechanism for MBO is described by a *localized transitions model*.

In the next two subsections we will provide an overview of these two types of models that have been proposed in the literature, in order to describe the properties of luminescence signals.

1.2.1 Delocalized Transition Models of TL

Figures 1.4 and 1.5 show several types of *delocalized models* that have been studied extensively in the literature. The arrows in these figures indicate electronic transitions, some of which involve transport of electrons and holes via the conduction and/or valence band. The simplest possible model that has been studied extensively

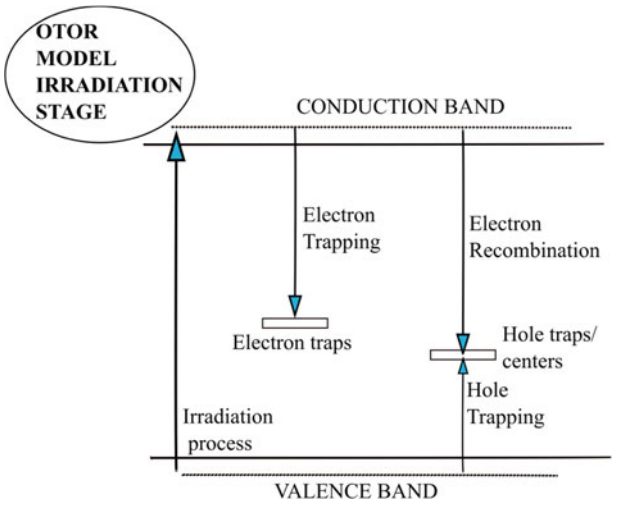

Fig. 1.4 The simplest OTOR model, showing the various electronic transitions during the irradiation stage. Irradiation creates electrons and holes in the conduction and valence bands, respectively. Electrons in the conduction band can subsequently either be trapped in electron traps, or they can be recombined with holes at the recombination centers/hole traps. Holes in the valence band can be trapped in the same recombination centers/hole traps

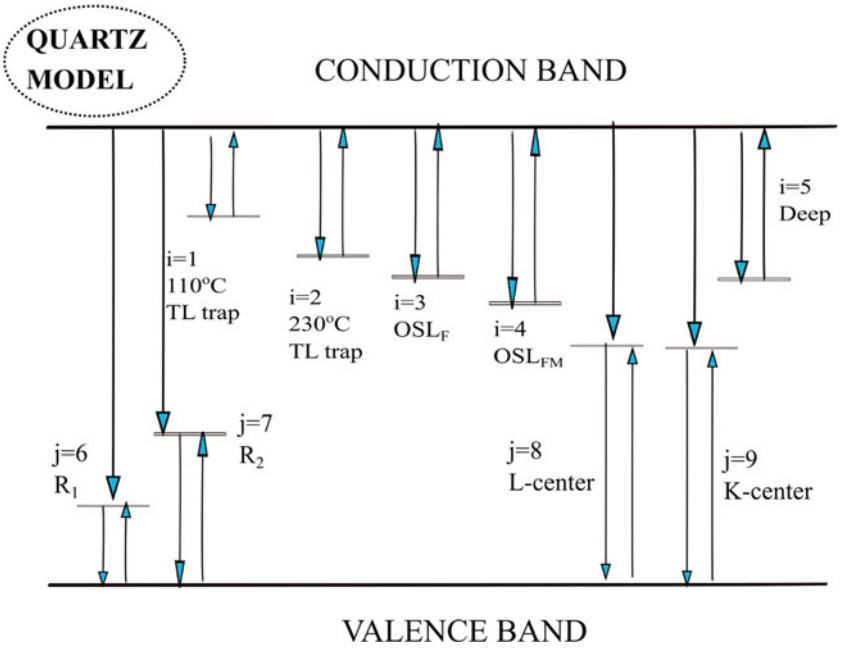

Fig. 1.5 Example of a complex *delocalized model* for quartz, involving multiple traps and centers (after Bailey [10]). Each arrow represents a transition between energy levels and the conduction and valence bands. These arrows also represent a mathematical term in a system of differential equations, as discussed in Chap. 11

in the literature consists of one trap and one recombination (OTOR) center and is shown in Fig. 1.4 for the irradiation process in a sample. The application of the OTOR model for TL and OSL data is presented in detail in Chaps. 2 and 3, in connection with analytical solutions based on the Lambert W function.

All differential equations in the models used to describe TL phenomena contain the Arrhenius thermal stimulation term $p(t)$ given by

$$p(t) = s \, \exp\left[\frac{-E}{k_B \, T(t)}\right] \tag{1.1}$$

where E (eV) is the thermal activation energy of the trap, $k_B = 8.617 \times 10^{-5}$ eV/K is the Boltzmann factor, $T(t)$ (K) is the time dependent temperature of the sample, and s (s^{-1}) is the associated frequency factor. Typical values of the frequency factor are $s = 10^8$–10^{12} s^{-1}, and for the activation energy $E = 0.7$–2 eV.

A more complex delocalized model that describes luminescence phenomena in quartz is shown in Fig. 1.5 and is presented in detail in Sect. 11.2 (Bailey [10]). This model is based on 5 electron traps indicated in the figure by the index $i = 1 - 5$ and on 4 hole traps/recombination centers indicated by the index $j = 6 - 9$ in this figure. Detailed applications of this model and its implementation in several R packages will be given in Chap. 11.

1.2.2 Localized Transition Models of TL

Figure 1.6 shows a comparison of the TL glow curves for the dosimetric materials MgB_4O_7:Dy,Na (MBO) and Al_2O_3:C (Pagonis et al. [119], Kitis et al. [81]). The shapes and widths of the main dosimetric peaks around 200 °C in these two materials are very different. The overall shape of the TL peak in Al_2O_3:C is asymmetric, while the TL peak in MBO is very nearly symmetric. The asymmetric shape for the peak in Al_2O_3:C is due to the luminescence mechanism involving first order kinetics (FOK) and *delocalized transitions*, as will be discussed in detail in Chap. 2.

The very wide TL peak observed for MBO is the result of a more complex underlying mechanism, which may involve an underlying distribution of activation energies and/or quantum tunneling mechanisms. These types of processes are discussed in Chap. 6. The luminescence mechanism in this material can be described by a *localized transition model*, similar to the one shown in Fig. 1.7.

In this book, we will look at several types of localized transition models that are organized in different chapters and sections, as shown in the chart of Fig. 1.8.

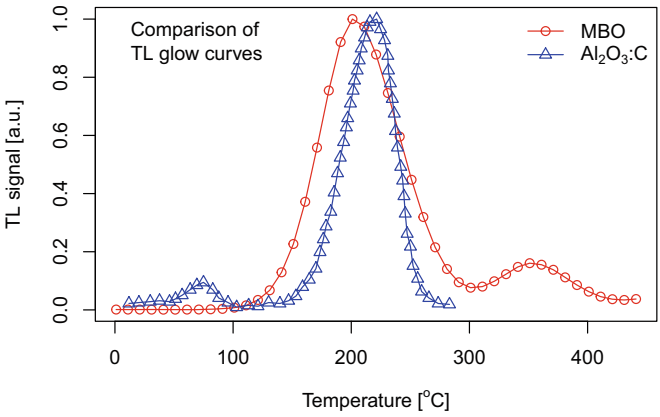

Fig. 1.6 Comparison of the TL glow curves MBO and Al_2O_3:C. The main dosimetric peak around 200 °C for MBO is very nearly symmetric, while for Al_2O_3:C the main peak is asymmetric. Notice also the difference between the widths of the main dosimetric peaks in the two materials. For more details, see Pagonis et al. [119] and Kitis et al. [81]

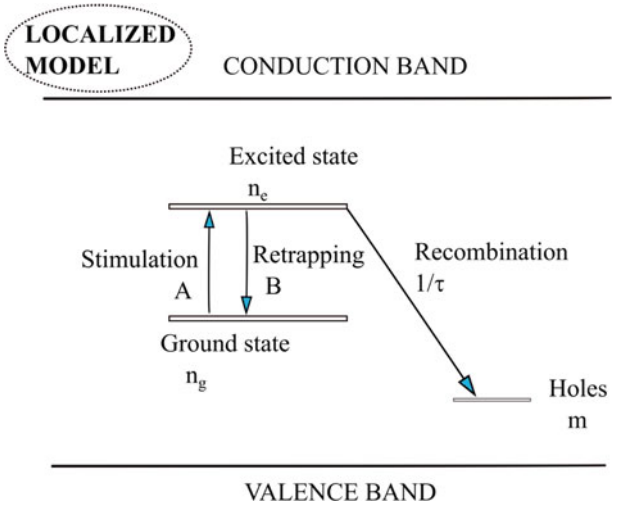

Fig. 1.7 A typical *localized transition model*, consisting of the ground state and the excited state of a trapped electron, and an additional energy level associated with a recombination center. Electrons are excited from the ground state (n_g) into the excited state (n_e) of the trap at a rate A and can also relax back into the ground state of the trap at the rate B. The transition indicated by the rate $1/\tau$ occurs from the excited state of the trap to an energy level of the recombination center (after Pagonis et al. [131])

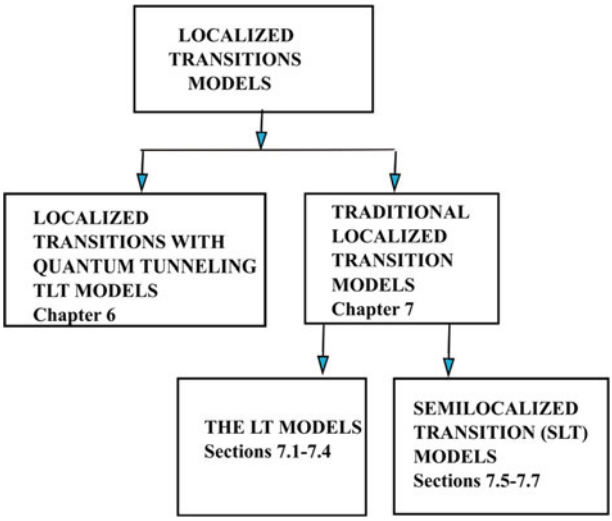

Fig. 1.8 The organization of localized transition models in Chaps. 6 and 7 of this book

1.3 Overview of Isothermal TL (ITL) Experiments and Models

When the thermal stimulation takes place at a constant temperature T_D, the stimulated luminescence signal is called *prompt isothermal decay* (PID), and the thermal stimulation function $p(t)$ is given by

$$p(t) = s \exp\left[\frac{-E}{k_B T_D}\right] \tag{1.2}$$

where E, s are the thermal kinetic parameters of the trap and k_B is the Boltzmann constant. An example of a PID curve is shown in Fig. 1.9a for the dosimetric material Magnesium tetraborate MgB_4O_7:Dy,Na (MBO) (Kitis et al. [81]). Figure 1.9b shows a series of remnant TL (RTL) glow curves for sample MBO, measured after an isothermal TL experiment for 500 s at the indicated temperatures. As the temperature of the isothermal TL experiment is increased, the maximum of the peaks decreases, and it also shifts toward higher temperatures. We will study this type of TL glow curve in connection with quantum tunneling and by using Monte Carlo methods in Chap. 6, and in connection with the R package *RLumCarlo* (Kreutzer et al. [87]).

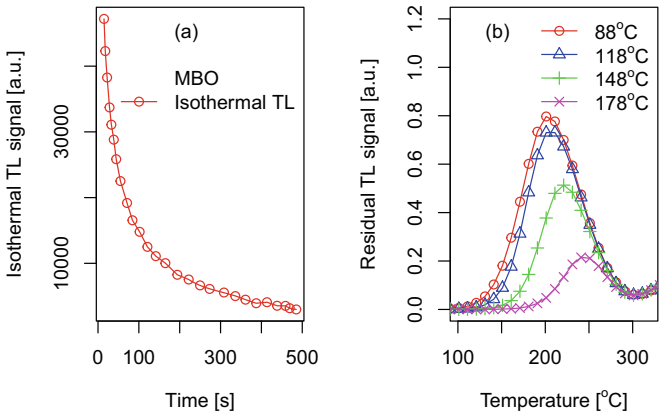

Fig. 1.9 (**a**) Isothermal TL signal for sample MBO and (**b**) a series of RTL glow curves, measured after an isothermal TL experiment for 500 s at the indicated temperatures. For more details, see Kitis et al. [81]

1.4 Overview of OSL, IRSL, and Their Models

When the stimulation of a sample is optical using visible light, one is dealing with *optically stimulated luminescence* (OSL). Typically, blue LEDs with a wavelength of 470 nm are used during these OSL experiments. When the stimulation is with visible light and also occurs with a source of constant light intensity, the stimulated luminescence is termed as *continuous wave optically stimulated luminescence* (CW-OSL), and the optical stimulation function $p(t)$ is given by

$$p(t) = \sigma\, I \tag{1.3}$$

where $\sigma\,(\mathrm{cm}^2)$ represents the optical cross section for the CW-OSL process, and $I\left(\mathrm{photons\,cm^{-2}\,s^{-1}}\right)$ represents the photon flux. The units of the stimulation rate $p(t)$ are s^{-1}.

In a similar manner, when the stimulation takes place with infrared photons, this process is called *infrared stimulated luminescence (IRSL)*. Typically, infrared LEDs with a wavelength of 850 nm are used during these IRSL experiments. In this case $\sigma\left(\mathrm{cm}^2\right)$ in Eq. (1.3) represents the corresponding optical cross section for the IRSL process. During CW-OSL or CW-IRSL experiments, the intensity of the light is kept constant, resulting in most cases in a monotonically decaying curve. An example of a CW-OSL curve measured with a constant optical excitation rate is shown in Fig. 1.10a, while Fig. 1.10b shows the CW-IRSL signal from the same sample (Kitis et al. [80]).

Figure 1.10 shows that the CW-OSL and CW-IRSL signals from the sample KT4 are very similar in shape. However, these signals are obtained with very different wavelengths of light (470 nm for blue light LEDs and 850 nm for infrared LEDs).

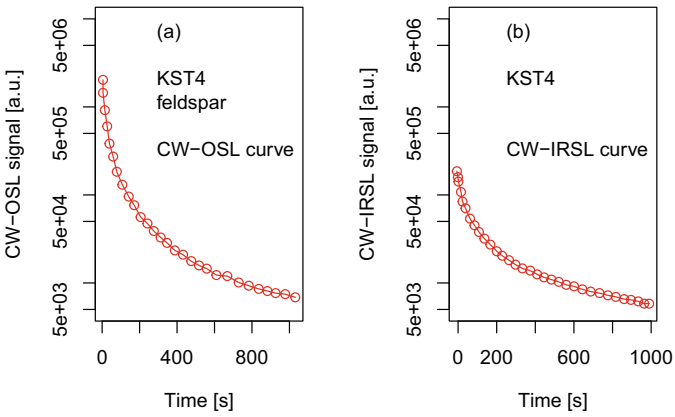

Fig. 1.10 Examples of (**a**) a CW-OSL curve and (**b**) a CW-IRSL curve, from the same geological feldspar sample KST4. For more details, see Kitis et al. [80]

Extensive research has shown that the mechanisms involved in the production of these signals are very different. In the case of the CW-OSL signal in Fig. 1.10a, the mechanism is believed to involve the conduction band and can be described by a *delocalized* model similar to the OTOR model shown in Fig. 1.4.

In the case of the CW-IRSL signal in Fig. 1.10b, the production mechanism is believed to involve localized energy levels located between the conduction and valence bands, as shown schematically previously in Fig. 1.7. Two versions of this type of *localized transition model* have been used in the literature, the simple localized transition (LT) model and the tunneling localized transition (TLT) model that is based on quantum mechanical tunneling processes. Both of these types of models are implemented in R in this book and are studied within the context of quantum tunneling, Monte Carlo methods, and the R package *RLumCarlo* in subsequent chapters.

Figure 1.11a shows the effect of different illumination powers on the CW-OSL signals for a quartz sample (Polymeris [154]). The stimulating power of the blue LEDs was varied in the range 50–90% of maximum power, and the data are normalized to the maximum intensity at time $t = 0$. The shape of the CW-OSL signal in Fig. 1.11a does not change significantly with the stimulating power of the blue LEDs. Figure 1.11b shows the CW-IRSL data obtained at different infrared light powers in the range 10–90% of maximum power, for a feldspar sample (Pagonis et al. [138]). This set of data has also been normalized to the maximum intensity, for comparison purposes. The shape of the CW-IRSL in Fig. 1.11b changes more significantly with the illumination power. This indicates either non-first order kinetics or the presence of multiple exponential components.

Note also that the OSL signal in Fig. 1.11a becomes negligible after 400 s of exposure to blue LEDs, while a large signal remains in Fig. 1.11b, even after exposure to 1000 s of infrared LED stimulation.

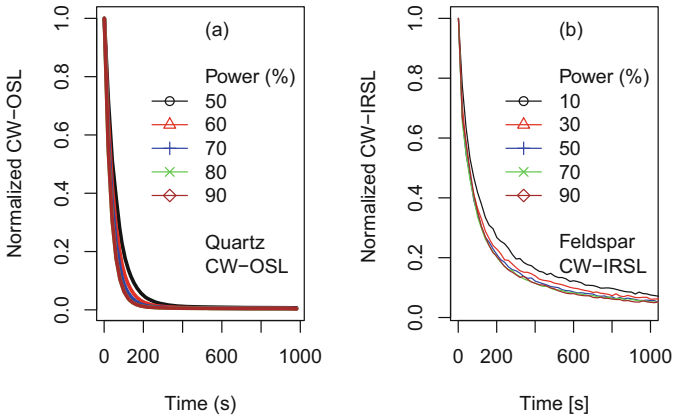

Fig. 1.11 (**a**) CW-OSL for quartz at different illumination powers in the range 50–90% of maximum power. (**b**) CW-IRSL signal at different illumination powers in the range 10–90% of maximum power, for a feldspar sample (laboratory code KST4). Both sets of data have been normalized to the maximum intensity. The shape of both signals changes with the illumination power. For more details, see Pagonis et al. [138] and Polymeris [154]

As we will discuss in later chapters, CW-OSL signals from quartz are described by *delocalized* transition models, while CW-IRSL signals from feldspars are described by *localized* transition models.

When the optical stimulation takes place using a source with an intensity that increases linearly with time, the stimulated luminescence is called *linearly modulated optically stimulated luminescence* (LM-OSL or LM-IRSL), and the stimulation rate $p(t)$ is given by

$$p(t) = \frac{\sigma\, I}{P}\, t \tag{1.4}$$

where σ, I have the same meaning as in Eq. (1.3), t is the elapsed time, and P (s) is the total illumination time.

During an LM-OSL or LM-IRSL experiment, the light intensity is recorded as a function of time, while increasing the stimulation linearly with time, thus obtaining a peak-shaped LM-OSL curve. The kinetics of such processes and the deconvolution of complex OSL signals into separate components by using available R packages are discussed in detail in Chap. 3.

Two examples of LM-OSL and LM-IRSL signals are shown in Fig. 1.12 for the dosimetric material CaF_2:N (Kitis et al. [78]) and for a K-feldspar (Bulur and Göksu [28]). The LM-OSL signal in Fig. 1.12a shows two peaks, and therefore, the luminescence mechanism for CaF_2:N involves at least two underlying components. By contrast, the LM-IRSL signal for the feldspar in Fig. 1.12b shows no apparent structure and may or may not involve a single luminescence component.

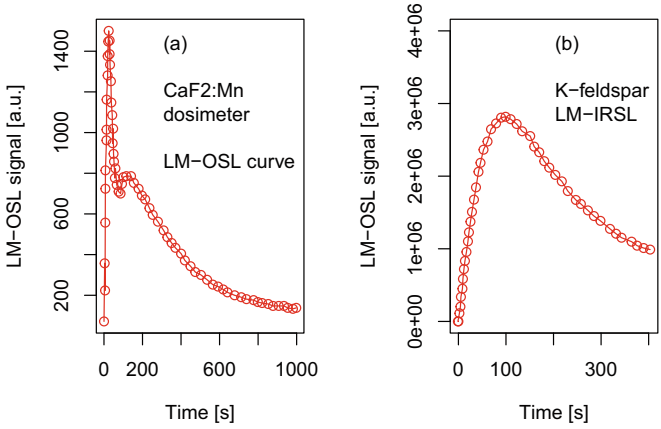

Fig. 1.12 Examples of (**a**) LM-OSL curve for the dosimetric material CaF_2:N (Kitis et al. [78]) and (**b**) LM-IRSL for a K-feldspar. For more details, see Bulur and Göksu [28]

1.5 Time-Resolved Luminescence Signals

In a time-resolved (TR) experiment, optical stimulation is used to separate in time the stimulation and emission of luminescence. The luminescence is stimulated using a brief light pulse (usually from bright LEDs), and the emission is monitored during the stimulation (when the LED is ON) and also during the relaxation stages of the experiment (when the LEDs are OFF). The details of TR experimental setups can be found in the review article by Chithambo et al. [41].

TR techniques have been very useful in the study of luminescence mechanisms for a variety of dosimetric materials. The optical stimulation is carried out in a pulsed mode, giving rise to *pulsed OSL* and *pulsed IRSL* signals (POSL and PIRSL).

Figure 1.13 shows two examples of TR-OSL curves, with very different time scales on the horizontal (time) axis. Figure 1.13a shows the TR-OSL signal from an Al_2O_3:C sample, while Fig. 1.13b shows the same experiment for a high purity synthetic quartz sample (Pagonis et al. [143]). The modeling of TR-OSL signals, and appropriate analysis of such experimental curves, is presented in Chap. 5.

Figure 1.14 shows two examples of TR-IRSL curves, from a microcline sample (laboratory code FL1, Pagonis et al. [120]). The modeling of these TR-IRSL signals, and appropriate analysis of such experimental curves, is presented in Chap. 5.

In many dosimetric materials, the pulsed OSL/IRSL signals depend strongly on the stimulation temperature. Specifically, one studies the temperature dependence of the luminescence intensity, as well as of the luminescence lifetimes determined from time-resolved luminescence spectra.

Figure 1.15 shows the TR-OSL signals from an Al_2O_3:C sample, measured at two different temperatures of 20 and 170 °C (Pagonis et al. [119]). One observes that as the stimulation temperature increases, the intensity of the TR-OSL signal

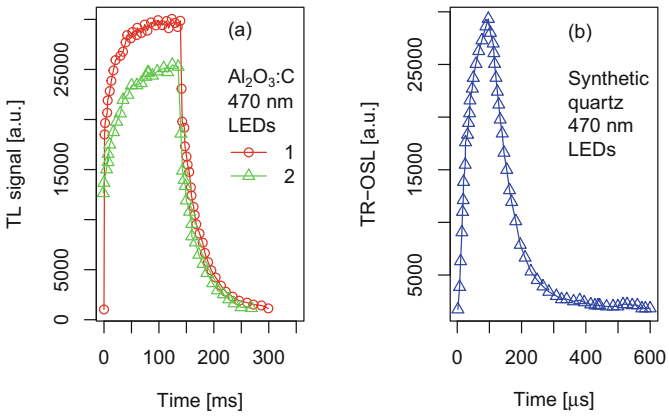

Fig. 1.13 Examples of TR-OSL curves for (**a**) Al_2O_3:C and (**b**) high purity synthetic quartz. Notice the very different time scales on the horizontal axis. The curves labeled 1 and 2 in (**a**) represent repeated measurements on the same sample, after the trapped electrons have been partially depleted. For more details, see Pagonis et al. [143]

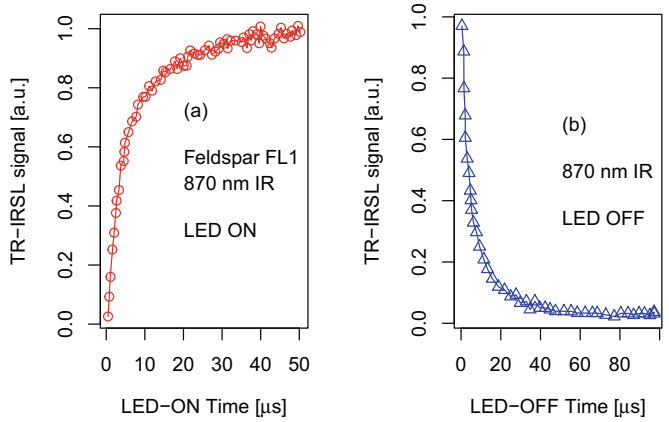

Fig. 1.14 Examples of TR-IRSL data for a feldspar sample FL1. (**a**) The TR-IRSL intensity as a function of the stimulation time during a 50 μs LED ON pulse. (**b**) The TR-IRSL intensity as a function of the stimulation time during the 100 μs LED OFF period. For more details, see Pagonis et al. [120]

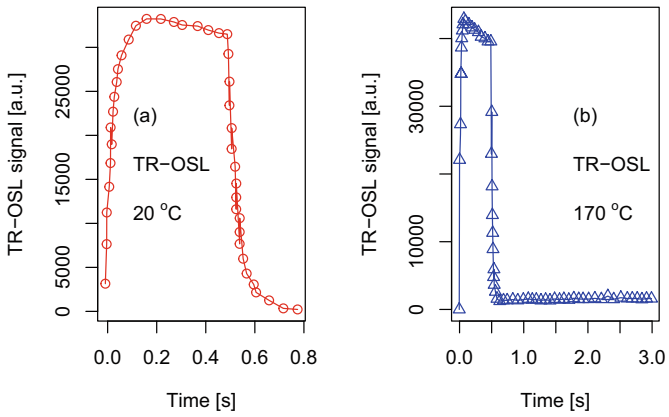

Fig. 1.15 Examples of TR-OSL data for Al_2O_3:C (**a**) at room temperature 20 °C and (**b**) at a stimulation temperature of 170 °C. For more details, see Pagonis et al. [119]

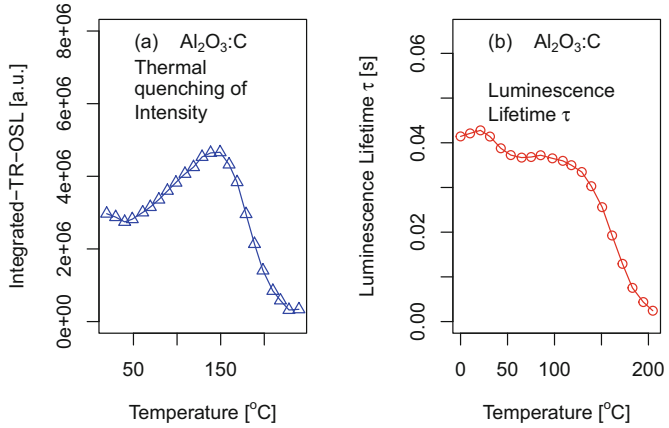

Fig. 1.16 Examples of TR-OSL data for Al_2O_3:C, showing the phenomenon of thermal quenching. (**a**) The integrated TR-OSL intensity as a function of the stimulation temperature. (**b**) The luminescence lifetime parameter τ as a function of the stimulation temperature. For more details, see Pagonis et al. [119]

varies, while at the same time the TR-OSL signal reaches its maximum value much faster. This phenomenon is referred to as *thermal quenching* of luminescence signals and will be discussed in some detail in Chap. 5.

Figure 1.16 shows the effect of thermal quenching on the TR-OSL signals from an Al_2O_3:C sample, as a function of the stimulation temperature (Pagonis et al. [119]). In Fig. 1.16a the intensity of the TR-OSL signal decreases as the stimulation temperature increases above 150 °C, while in Fig. 1.16b the lifetime τ of the TR-OSL signals overall decreases from about 40 ms at room temperature, to a few ms at stimulation temperatures higher than 200 °C.

1.6 Overview of ESR and OA Experiments: Correlations with Luminescence Signals

In this section we discuss briefly optical absorption (OA) and electron spin resonance (ESR) experiments and point out their relationship to TL and OSL data. For a more complete review of these types of experiments in connection with TL/OSL data, the reader is referred to the ESR review paper by Trompier et al. [181] and also to the extensive list of references in the book by Chen and Pagonis [38].

ESR and OA experiments are often measured simultaneously with TL and/or OSL with the same sample. These combined types of experiments produce important information about the underlying luminescence mechanisms, as well as about the nature of the trapping and luminescence centers (see, e.g. the quartz study by Yang and McKeever [193]).

The absorption technique of electron spin (paramagnetic) resonance (ESR, EPR) is used for the study of materials that exhibit paramagnetism because of the magnetic moment of unpaired electrons. ESR spectra are usually presented as plots of the absorption or dispersion of the energy of an oscillating magnetic field of fixed radio frequency, versus the intensity of an applied static magnetic field. Among the wide variety of paramagnetic substances to which ESR spectroscopy has been applied, the one that is of interest in the present context is that of impurity centers in solids, mainly single crystals. The same impurity centers may be associated with TL or OSL, either acting as the charge carrier traps or as recombination centers. They may also be responsible for optical absorption.

Since ESR is normally capable of identifying the impurities in the crystal, in cases where the simultaneous TL-ESR measurements show a direct relation between the two phenomena, the identification by ESR may serve as a direct proof for the identity of the impurity involved in the luminescence process. In many cases the OA and/or the ESR signal show a decrease at a certain temperature range, where the trapping state becomes unstable. The instability may be associated with either the thermal release of charge carriers from the paramagnetic impurity, or, alternatively, the filling of paramagnetic impurities that serve as TL recombination centers. In general, it is expected that the TL peak will resemble the negative derivative of the ESR signal, with a close resemblance to OA (Chen and Pagonis [38]).

Figure 1.17 shows an example of the dose dependence of an ESR signal in quartz from Duval [46]. This author measured the dose response curves of the Al center for 15 sedimentary quartz samples from the Iberian Peninsula. The samples were irradiated up to a maximum dose of 23–40 kGy. It was found that the ESR signal grows almost linearly with the absorbed dose for doses above about 4 kGy.

The dose responses of TL, OSL, OA, and ESR signals exhibit nonlinear regions, associated with the phenomena of superlinearity and sublinearity. These are discussed in detail in Chap. 4, in connection with recent theoretical research involving the Lambert W function (Pagonis et al. [135]).

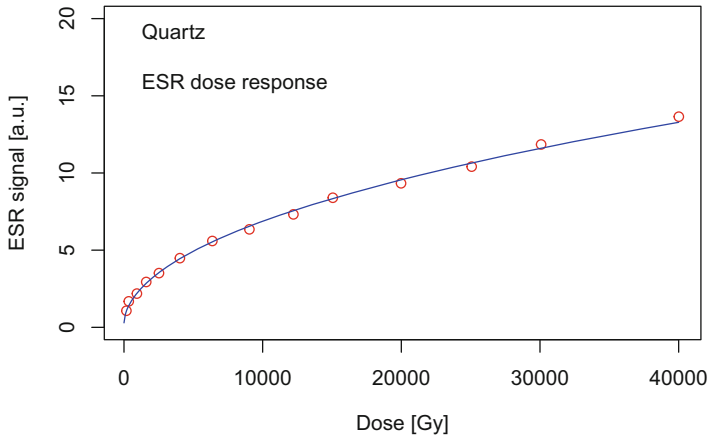

Fig. 1.17 Example of the dose response of ESR data from quartz. Redrawn from Pagonis et al. [135], original data from Duval [46]

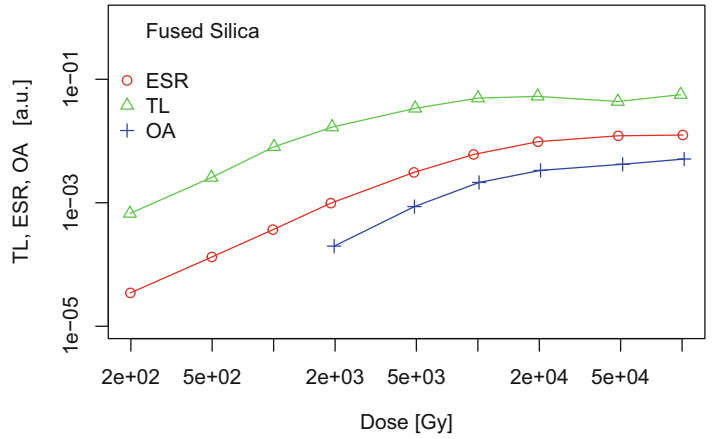

Fig. 1.18 Measurements of TL, ESR, and OA signals as a function of the irradiation dose, from a single sample of fused silica. Note the log scale in both axes. For more details, see Pagonis et al. [136], original data from Wieser et al. [189]

Figure 1.18 shows simultaneous measurements and possible correlations between the TL, ESR, and OA signals from a sample of fused silica (Wieser et al. [189]). This type of multifaceted experiment can be very useful in identifying the source of the various luminescence signals, i.e. the nature of the traps and centers in the dosimetric material.

1.7 What Information Can We Extract from TL, OSL, and TR Luminescence Signals?

The luminescence signals discussed in this chapter and in the rest of this book are obviously complex. The fundamental question for researchers is what kind of information they can extract from the experimental curves, and how.

In general, researchers would like to extract the following specific information:

- The intensity of the light emitted during each stimulated luminescence effect, as a function of time or as a function of temperature.
- The *dose response*, i.e. the intensity of the light emitted as a function of irradiation dose.
- The basic physical parameters of the energy level responsible for the emission of light. For thermally stimulated processes, these parameters are the activation energy E and the frequency factor s. For optically stimulated processes, they are the cross section σ for the corresponding process.
- Information on the physical mechanism behind the observed luminescence signals, and on the various processes involved.
- Information on whether the delocalized conduction and valence bands are involved in the luminescence processes, and whether localized energy transitions play a role in the production of the luminescence signals.

Luminescence signals from dosimetric materials are characterized by the presence of several components, originating from different traps or centers. These signals vary according to the preconditioning of the samples (irradiation dose, prior optical and thermal stimulation, radiation quality) and are described mathematically by phenomenological models based usually on systems of coupled differential equations.

As discussed in this chapter, two types of models that have been used extensively in the literature are *delocalized models* based on transitions involving the conduction and valence bands, and *localized models* usually involving different energy levels of the traps/centers. For a comprehensive historical summary of various types of luminescence models, the reader is referred for example to the book by Chen and Pagonis [38], and the review paper by McKeever and Chen [112]. The details of these models and their implementation with R are given in several later chapters.

The main goals of *modeling* studies are:

- to provide a quantitative description of these dosimetric signals;
- to develop methods for the accurate evaluation of parameters characterizing traps and centers;
- to search for general models that explain the behavior of preconditioned samples;
- to help researchers understand the underlying luminescence production mechanisms.

References

1. G Adamiec, R M Bailey, X L Wang, and A G Wintle. The mechanism of thermally transferred optically stimulated luminescence in quartz. *Journal of Physics D: Applied Physics*, 41(13):135503, 2008.
2. G Adamiec, A Bluszcz, R Bailey, and M Garcia-Talavera. Finding model parameters: Genetic algorithms and the numerical modelling of quartz luminescence. *Radiation Measurements*, 41(7–8):897–902, 2006.
3. G Adamiec, M Garcia-Talavera, R M Bailey, and P I de La Torre. Application of a genetic algorithm to finding parameter values for numerical simulation of quartz luminescence. *Geochronometria*, 23:9–14, 2004.
4. M S Akselrod, N A Larsen, V Whitley, and S W S McKeever. Thermal quenching of F-center luminescence in Al_2O_3:C. *Journal of Applied Physics*, 84(6):3364–3373, 1998.
5. L J S Allen. *An introduction to stochastic processes with applications to biology*. Chapman and Hall/CRC, 2010.
6. V Anechitei-Deacu, A Timar-Gabor, K J Thomsen, J-P Buylaert, M Jain, M Bailey, and A S Murray. Single and multi-grain OSL investigations in the high dose range using coarse quartz. *Radiation Measurements*, 120:124–130, 2018.
7. M Autzen, A S Murray, G. Guérin, L. Baly, C. Ankjærgaard, M. Bailey, M. Jain, and J.-P. Buylaert. Luminescence dosimetry: Does charge imbalance matter? *Radiation Measurements*, 120:26–32, 2018.
8. R Bailey. Simulations of variability in the luminescence characteristics of natural quartz and its implications for estimates of absorbed dose. *Radiation Protection Dosimetry*, 100:33–38, 2002.
9. R Bailey. Paper I - Simulation of dose absorption in quartz over geological timescales and its implications for the precision and accuracy of optical dating. *Radiation Measurements*, 38:299–310, 2004.
10. R M Bailey. Towards a general kinetic model for optically and thermally stimulated luminescence of quartz. *Radiation Measurements*, 33(1):17–45, 2001.
11. R M Bailey, B W Smith, and E J Rhodes. Partial bleaching and the decay form characteristics of quartz OSL. *Radiation Measurements*, 27(2):123–136, 1997.
12. I K Bailiff. The pre-dose technique. *Radiation Measurements*, 23(2):471–479, 1994.
13. H G Balian and N W Eddy. Figure-of-merit (FOM), an improved criterion over the normalized chi-squared test for assessing goodness-of-fit of gamma-ray spectral peaks. *Nuclear Instruments and Methods*, 145:389–395, 1977.
14. G W Berger. Regression and error analysis for a saturating-exponential-plus-linear model. *Ancient TL*, 8(3):23–25, 1990.

© The Author(s), under exclusive license to Springer Nature Switzerland AG 2021

V. Pagonis, *Luminescence*, Use R!, https://doi.org/10.1007/978-3-030-67311-6

15. G W Berger and R Chen. Error analysis and modelling of double saturating exponential dose response curves from SAR OSL dating. *Ancient TL*, 29(1):9–14, 2011.
16. R H Biswas, F Herman, G E King, and J Braun. Thermoluminescence of feldspar as a multi-thermochronometer to constrain the temporal variation of rock exhumation in the recent past. *Earth and Planetary Science Letters*, 495:56–68, 2018.
17. A Bluszcz. Exponential function fitting to TL growth data and similar applications. *Geochronometria*, 13:135–141, 1996.
18. A Bluszcz and G Adamiec. Application of differential evolution to fitting OSL decay curves. *Radiation Measurements*, 41(7–8):886–891, 2006.
19. L Bøetter-Jensen, S W S McKeever, and A G Wintle. *Optically Stimulated Luminescence Dosimetry*. Elsevier Science, 2003.
20. A J J Bos. Thermoluminescence as a research tool to investigate luminescence mechanisms. *Materials (Basel, Switzerland)*, 10, November 2017.
21. A J J Bos, T M Piters, J M Gómez-Ros, and A Delgado. An intercomparison of glow curve analysis computer programs: I. synthetic glow curves. *Radiation protection dosimetry*, 47:473–477, 1993.
22. J J Bosken and C Schmidt. Direct and indirect luminescence dating of tephra: A review. *Journal of Quaternary Science*, 35(1–2):39–53, 2020.
23. S G E Bowman and R Chen. Superlinear filling of traps in crystals due to competition during irradiation. *Journal of Luminescence*, 18–19:345–348, 1979.
24. N D Brown, E J Rhodes, and T M Harrison. Using thermoluminescence signals from feldspars for low-temperature thermochronology. *Quat. Geochronol.*, 42:31–41, 2017.
25. R K Bull. Kinetics of the localised transition model for thermoluminescence. *Journal of Physics D: Applied Physics*, 22(9):1375–1379, sep 1989.
26. E Bulur. An alternative technique for optically stimulated luminescence (OSL) experiment. *Radiation Measurements*, 26(5):701–709, 1996.
27. E Bulur. A simple transformation for converting CW-OSL curves to LM-OSL curves. *Radiation Measurements*, 32(2):141–145, 2000.
28. E Bulur and H Y Göksu. Infrared (IR) stimulated luminescence from feldspars with linearly increasing excitation light intensity. *Radiation Measurements*, 30:505–512, 1999.
29. E Bulur and A Yeltik. Optically stimulated luminescence from BeO ceramics: An LM-OSL study. *Radiation Measurements*, 45:29–34, 2010.
30. I F Chang and P Thioulouse. Treatment of thermostimulated luminescence, phosphorescence, and photostimulated luminescence with a tunneling theory. *Journal of Applied Physics*, 53(8):5873–5875, 1982.
31. R Chen. Glow curves with general order kinetics. *Journal of The Electrochemical Society*, 116:1254, 1969.
32. R Chen. On the calculation of activation energies and frequency factors from glow curves. *Journal of Applied Physics*, 40:570–585, 1969.
33. R Chen and Y Kirsh. *Analysis of Thermally Stimulated Processes*. Oxford: Pergamon Press., 1981.
34. R Chen, N Kristianpoller, Z Davidson, and R Visocekas. Mixed first and second order kinetics in thermally stimulated processes. *Journal of Luminescence*, 23:293–303, 1981.
35. R Chen, J L Lawless, and V Pagonis. Competition between long time excitation and fading of thermoluminescence (TL) and optically stimulated luminescence (OSL). *Radiation Measurements*, 136:106422, 2020.
36. R Chen and S W S McKeever. Characterization of nonlinearities in the dose dependence of thermoluminescence. *Radiation Measurements*, 23(4):667–673, 1994.
37. R Chen and S W S McKeever. *Theory of thermoluminescence and related phenomena*. World Scientific, Singapore, 1997.
38. R Chen and V Pagonis. *Thermally and Optically Stimulated Luminescence: A Simulation Approach*. John Wiley & Sons, Chichester, 2011.
39. M L Chithambo. The analysis of time-resolved optically stimulated luminescence: I. theoretical considerations. *Journal of Physics D: Applied Physics*, 40(7):1874, 2007.

40. M L Chithambo. The analysis of time-resolved optically stimulated luminescence: II. computer simulations and experimental results. *Journal of Physics D: Applied Physics*, 40(7):1880, 2007.
41. M L Chithambo, C Ankjærgaard, and V Pagonis. Time-resolved luminescence from quartz: An overview of contemporary developments and applications. *Physica B: Condensed Matter*, 481:8–18, 2016.
42. M L Chithambo and R B Galloway. A pulsed light-emitting-diode system for stimulation of luminescence. *Measurement Science and Technology*, 11(4):418–424, mar 2000.
43. R J Clark and I K Bailiff. Fast time-resolved luminescence emission spectroscopy in some feldspars. *Radiation Measurements*, 29(5):553–560, 1998.
44. R M Corless, G H Gonnet, D G E Hare, D J Jerey, and D E Knuth. On the Lambert W function. *Advances in Computational Mathematics*, 5:329–359, 1996.
45. R M Corless, D J Jerey, and D E Knuth. A sequence series for the Lambert W function. *In Proceedings of the International Symposium on Symbolic and Algebraic Computation , ISSAC*, pages 133–140, 1997.
46. M Duval. Dose response curve of the ESR signal of the aluminum center in quartz grains extracted from sediment. *Ancient TL*, 30(2):1–9, 2012.
47. J M Edmund. *Effects of temperature and ionization density in medical luminescence dosimetry using Al2O3:C (PhD Thesis, Riso, Denmark)*. PhD thesis, Risø National Laboratory, 2007. Riso-PhD-38(EN).
48. J Friedrich, S Kreutzer, and C Schmidt. Solving ordinary differential equations to understand luminescence: 'RLumModel', an advanced research tool for simulating luminescence in quartz using R . *Quaternary Geochronology*, 35:88–100, 2016.
49. J Friedrich, V Pagonis, R Chen, S Kreutzer, and C Schmidt. Quartz radiofluorescence: a modelling approach. *Journal of Luminescence*, 186:318–325, 2017.
50. M Fuchs, S Kreutzer, D Rousseau, P Antoine, C Hatté, F Lagroix, O Moine, C Gauthier, J Svoboda, and L Lisá. The loess sequence of Dolní Věstonice, Czech Republic: A new OSL-based chronology of the last climatic cycle. *Boreas*, 42(3):664–677, 2013.
51. G F J Garlick and A F Gibson. The electron trap mechanism of luminescence in sulphide and silicate phosphors. *Proceedings of the Physical Society*, 60:574–590, 1948.
52. J M Gómez-Ros and G Kitis. Computerized glow-curve deconvolution using mixed and general order kinetics. *Radiation Protection Dosimetry*, 101:47–52, 2002.
53. H Gould, J Tobochnik, D C Meredith, S E Koonin, S R McKay, and W Christian. *An Introduction to Computer Simulation Methods: Applications to Physical Systems, 2nd Edition*, volume 10. Addison-Wesley;, 1996.
54. G Grolemund. *Hands-on programming with R: write your own functions and simulations*. "O'Reilly Media, Inc.", 2014.
55. A Halperin and A A Braner. Evaluation of thermal activation energies from glow curves. *Physical Review*, 117:408–415, 1960.
56. A Halperin and R Chen. Thermoluminescence of semiconducting diamonds. *Phys. Rev.*, 148:839–845, Aug 1966.
57. Y Horowitz, E Fuks, H Datz, L Oster, J Livingstone, and A Rosenfeld. Mysteries of LiF TLD response following high ionization density irradiation: Glow curve shapes, dose response, the unified interaction model and modified track structure theory. *Radiation Measurements*, 46(12):1342–1348, 2011.
58. Y S Horowitz. The theoretical and microdosimetric basis of thermoluminescence and applications to dosimetry. *Physics in medicine and biology*, 26:765–824, Sep 1981.
59. D J Huntley. An explanation of the power-law decay of luminescence. *Journal of Physics: Condensed Matter*, 18(4):1359, 2006.
60. D J Huntley and M Lamothe. Ubiquity of anomalous fading in K-feldspars and the measurement and correction for it in optical dating. *Canadian Journal of Earth Sciences*, 38(7):1093–1106, 2001.
61. D J Huntley and Olav B Lian. Some observations on tunnelling of trapped electrons in feldspars and their implications for optical dating. *Quaternary Science Reviews*, 25(19–20):2503–2512, 2006.

62. M Jain, B Guralnik, and M T Andersen. Stimulated luminescence emission from localized recombination in randomly distributed defects. *Journal of Physics: Condensed Matter*, 24(38):385402, 2012.
63. M Jain, R Sohbati, B Guralnik, A S Murray, M Kook, T Lapp, A K Prasad, K J Thomsen, and J P Buylaert. Kinetics of infrared stimulated luminescence from feldspars. *Radiation Measurements*, 81:242–250, 2015.
64. R H Kars and J Wallinga. IRSL dating of K-feldspars: Modelling natural dose response curves to deal with anomalous fading and trap competition. *Radiation Measurements*, 44(5):594–599, 2009.
65. R Katz. Track structure theory in radiobiology and in radiation detection. *Nuclear Track Detection*, 2(1):1–28, 1978.
66. G E King, B Guralnik, P G Valla, and F Herman. Trapped-charge thermochronometry and thermometry: A status review. *Chemical Geology*, 44:3–17, 2016.
67. G E King, F Herman, R Lambert, P G Valla, and B Guralnik. Multi OSL thermochronometry of feldspar. *Quaternary Geochronology*, 33:76–87, 2016.
68. G Kitis, C Furetta, and V Pagonis. Mixed-order kinetics model for optically stimulated luminescence. *Modern Physics Letters B*, 23(27):3191–3207, 2009.
69. G Kitis and J M Gómez-Ros. Glow curve deconvolution functions for mixed order kinetics and a continuous trap distribution. *Nucl. Instrum. Methods A 440*, 440:224–231, 1999.
70. G Kitis, J M Gómez-Ros, and J W N Tuyn. Thermoluminescence glow curve deconvolution functions for first, second and general order kinetics. *J. Phys. D: Appl. Phys.*, 31:2666–2646, 1998.
71. G Kitis, N Kiyak, G S Polymeris, and N C Tsirliganis. The correlation of fast OSL component with the TL peak at in quartz of various origins. *Journal of Luminescence*, 130:298–303, 2010.
72. G Kitis and V Pagonis. Computerized curve deconvolution analysis for LM-OSL. *Radiation Measurements*, 43:737–741, 2008.
73. G Kitis and V Pagonis. Analytical solutions for stimulated luminescence emission from tunneling recombination in random distributions of defects. *Journal of Luminescence*, 137:109–115, 2013.
74. G Kitis and V Pagonis. Properties of thermoluminescence glow curves from tunneling recombination processes in random distributions of defects. *Journal of Luminescence*, 153:118–124, 2014.
75. G Kitis and V Pagonis. Localized transition models in luminescence: A reappraisal. *Nuclear Instruments and Methods in Physics Research Section B: Beam Interactions with Materials and Atoms*, 432:13–19, 2018.
76. G Kitis, V Pagonis, H Carty, and E Tatsis. Detailed kinetic study of the thermoluminescence glow curve of synthetic quartz. *Radiation protection dosimetry*, 100(1–4):225–228, 2002.
77. G Kitis, V Pagonis, and R Chen. Comparison of experimental and modelled quartz thermal-activation curves obtained using multiple-and single-aliquot procedures. *Radiation Measurements*, 41:910–916, 2006.
78. G Kitis, G S Polymeris, and V Pagonis. Stimulated luminescence emission: From phenomenological models to master analytical equations. *Applied Radiation and Isotopes*, 153:108797, 2019.
79. G Kitis, G S Polymeris, V Pagonis, and N C Tsirliganis. Thermoluminescence response and apparent anomalous fading factor of Durango fluorapatite as a function of the heating rate. *Physica Status Solidi (A) Applications and Materials Science*, 203(15):3816–3823, 2006.
80. G Kitis, G S Polymeris, E Sahiner, N Meric, and V Pagonis. Influence of the infrared stimulation on the optically stimulated luminescence in four K-feldspar samples. *Journal of Luminescence*, 176:32–39, 2016.
81. G Kitis, G S Polymeris, I K Sfampa, M Prokic, N Meriç, and V Pagonis. Prompt isothermal decay of thermoluminescence in Mg_4BO_7: Dy, Na and Li_4BO_7:Cu,In dosimeters. *Radiation Measurements*, 84:15–25, 2016.
82. G Kitis and N D Vlachos. General semi-analytical expressions for TL, OSL and other luminescence stimulation modes derived from the OTOR model using the Lambert W-function. *Radiation Measurements*, 48:47–54, 2013.

83. M J Klein. Principle of detailed balance. *Phys. Rev.*, 97:1446–1447, Mar 1955.
84. D K Koul, V Pagonis, and P Patil. Reliability of single aliquot regenerative protocol (SAR) for dose estimation in quartz at different burial temperatures: A simulation study. *Radiation Measurements*, 91:28–35, 2016.
85. S Kreutzer, Christoph Burow, Michael Dietze, Margret C Fuchs, Manfred Fischer, and Christoph Schmidt. Software in the context of luminescence dating: status, concepts and suggestions exemplified by the R package Luminescence. *Ancient TL*, 35(2), 2017.
86. S Kreutzer, M Dietze, C Burow, M C Fuchs, C Schmidt, M Fischer, and J Friedrich. Luminescence: Comprehensive Luminescence Dating Data Analysis. *CRAN*, version 0.7.5, 2017. Developer version on GitHub: https://github.com/R-Lum/Luminescence.
87. S Kreutzer, J Friedrich, V Pagonis, and C Schmidt. Rlumcarlo: Tedious features-fine examples. *Simulation*, 1:1–1E5, 2021.
88. S Kreutzer, C Schmidt, M C Fuchs, M Dietze, M Fischer, and M Fuchs. Introducing an R package for luminescence dating analysis. *Ancient TL*, 30(1):1–8, 2012.
89. R N Kulkarni. The development of the Monte Carlo method for the calculation of the thermoluminescence intensity and the thermally stimulated conductivity. *Radiation protection dosimetry*, 51(2):95–105, 1994.
90. David P L and K Binder. *A guide to Monte Carlo simulations in statistical physics*. Cambridge University Press, 2014.
91. M Lamothe, M Auclair, C Hamzaoui, and S Huot. Towards a prediction of long-term anomalous fading of feldspar IRSL. *Radiation Measurements*, 37(4):493–498, 2003.
92. A Larsen, S Greilich, M Jain, and A S Murray. Developing a numerical simulation for fading in feldspar. *Radiation Measurements*, 44(5):467–471, 2009.
93. J L Lawless, R Chen, and V Pagonis. On the theoretical basis for the duplicitous thermoluminescence peak. *Journal of Physics D: Applied Physics*, 42(15), 2009.
94. J L Lawless, R Chen, and V Pagonis. Sublinear dose dependence of thermoluminescence and optically stimulated luminescence prior to the approach to saturation level. *Radiation Measurements*, 44(5):606–610, 2009.
95. J L Lawless, R Chen, and V Pagonis. Inherent statistics of glow curves from small samples and single grains. *Journal of Luminescence*, 226:117389, 2020.
96. P W Levy. Overview Of Nuclear Radiation Damage Processes: Phenomenological Features Of Radiation Damage In Crystals And Glasses. In Paul W. Levy, editor, *Radiation Effects on Optical Materials*, volume 0541, pages 2–24. International Society for Optics and Photonics, SPIE, 1985.
97. B Li, Z Jacobs, and R G Roberts. Investigation of the applicability of standardised growth curves for OSL dating of quartz from Haua Fteah cave, Libya. *Quaternary Geochronology*, 35:1–15, 2016.
98. B Li and S H Li. Investigations of the dose-dependent anomalous fading rate of feldspar from sediments. *Journal of Physics D: Applied Physics*, 41(22):225502, oct 2008.
99. S E Lowick, F Preusser, and A G Wintle. Investigating quartz optically stimulated luminescence dose response curves at high doses. *Radiation Measurements*, 45(9):975–984, 2010.
100. A Mandowski. The theory of thermoluminescence with an arbitrary spatial distribution of traps. *Radiation Protection Dosimetry*, 100:115–118, 2002.
101. A Mandowski. Semi-localized transitions model for thermoluminescence. *Journal of Physics D: Applied Physics*, 38:17, 2005.
102. A Mandowski. Calculation and properties of trap structural functions for various spatially correlated systems. *Radiation protection dosimetry*, 119:85–88, 2006.
103. A Mandowski. How to detect trap cluster systems? *Radiation Measurements*, 43(2):167–170, 2008.
104. A Mandowski and A J J Bos. Explanation of anomalous heating rate dependence of thermoluminescence in YPO4:Ce^{3+}, Sm^{3+} based on the semilocalized transition (SLT) model. *Radiation Measurements*, 46:1376–1379, 2011.
105. A Mandowski and J Świątek. Monte Carlo simulation of thermally stimulated relaxation kinetics of carrier trapping in microcrystalline and two-dimensional solids. *Philosophical Magazine B*, 65:729–732, 1992.

106. A Mandowski and J Świątek. Monte Carlo simulation of TSC and TL in spatially correlated systems. In *Electrets, 1994.(ISE 8), 8th International Symposium on*, pages 461–466. IEEE, 1994.
107. A Mandowski and J Świątek. On the influence of spatial correlation on the kinetic order of TL. *Radiation protection dosimetry*, 65:25–28, 1996.
108. A Mandowski and J Świątek. The kinetics of trapping and recombination in low dimensional structures. *Synthetic Metals*, 109:203–206, 2000.
109. A Mandowski and Józef Świątek. Thermoluminescence and trap assemblies: results of Monte Carlo calculations. *Radiation Measurements*, 29:415–419, 1998.
110. C E May and J A Partridge. Thermoluminescent kinetics of alpha-irradiated alkali halides. *The Journal of Chemical Physics*, 40(5):1401–1409, 1964.
111. S W S McKeever. Thermoluminescence of solids. Cambridge University Press, 1985.
112. S W S McKeever and R Chen. Luminescence models. *Radiation Measurements*, 27(5):625–661, 1997.
113. E F Mische and S W S McKeever. Mechanisms of Supralinearity in Lithium Fluoride Thermoluminescence Dosemeters. *Radiation Protection Dosimetry*, 29(3):159–175, 11 1989.
114. P Morthekai, J Thomas, M S Pandian, V Balaram, and A K Singhvi. Variable range hopping mechanism in band-tail states of feldspars: A time-resolved irsl study. *Radiation Measurements*, 47(9):857–863, 2012.
115. R Nanjundaswamy, K Lepper, and SWS McKeever. Thermal quenching of thermoluminescence in natural quartz. *Radiation protection dosimetry*, 100(1–4):305–308, 2002.
116. S V Nikiforov, V S Kortov, and M G Kazantseva. Simulation of the superlinearity of dose characteristics of thermoluminescence of anion-defective aluminum oxide. *Physics of the Solid State*, 56(3):554–560, March 2014.
117. S V Nikiforov, I I Milman, and V S Kortov. Thermal and optical ionization of F-centers in the luminescence mechanism of anion-defective corundum crystals. *Radiation Measurements*, 33(5):547–551, 2001. Proceedings of the International Symposium on Luminescent Detectors and Transformers of Ionizing Radiation.
118. A S Novozhilov, G P Karev, and E V Koonin. Biological applications of the theory of birth-and-death processes. *Briefings in Bioinformatics*, 7(1):70–85, 03 2006.
119. V Pagonis, C Ankjærgaard, M Jain, and R Chen. Thermal dependence of time-resolved blue light stimulated luminescence in Al_2O_3:C. *Journal of Luminescence*, 136:270–277, 2013.
120. V Pagonis, C Ankjærgaard, M Jain, and M L Chithambo. Quantitative analysis of time-resolved infrared stimulated luminescence in feldspars. *Physica B: Condensed Matter*, 497:78–85, 2016.
121. V Pagonis, C Ankjærgaard, A S Murray, M Jain, R Chen, J Lawless, and S Greilich. Modelling the thermal quenching mechanism in quartz based on time-resolved optically stimulated luminescence. *Journal of Luminescence*, 130(5):902–909, 2010.
122. V Pagonis, L Blohm, M Brengle, G Mayonado, and P Woglam. Anomalous heating rate effect in thermoluminescence intensity using a simplified semi-localized transition (SLT) model. *Radiation Measurements*, 51–52:40–47, 2013.
123. V Pagonis and N Brown. On the unchanging shape of thermoluminescence peaks in preheated feldspars: Implications for temperature sensing and thermochronometry. *Radiation Measurements*, 2019.
124. V Pagonis, N Brown, G S Polymeris, and G Kitis. Comprehensive analysis of thermoluminescence signals in Mg_4BO_7: Dy, Na dosimeter. *Journal of Luminescence*, 213:334–342, 2019.
125. V Pagonis and R Chen. Monte Carlo simulations of TL and OSL in nanodosimetric materials and feldspars. *Radiation Measurements*, 81:262–269, 2015.
126. V Pagonis, R Chen, and G Kitis. On the intrinsic accuracy and precision of luminescence dating techniques for fired ceramics. *Journal of Archaeological Science*, 38(7):1591–1602, 2011.
127. V Pagonis, R Chen, C Kulp, and G Kitis. An overview of recent developments in luminescence models with a focus on localized transitions. *Radiation Measurements*, 106:3–12, 2017.

128. V Pagonis, R Chen, and J L Lawless. A quantitative kinetic model for Al2O3: C: TL response to ionizing radiation. *Radiation Measurements*, 42(2):198–204, 2007.
129. V Pagonis, R Chen, Maddrey J W, and Sapp B. Simulations of time-resolved photoluminescence experiments in Al_2O_3:C. *Journal of Luminescence*, 131(5):1086–1094, 2011.
130. V Pagonis, Gochnour E, Hennessey M, and Knower C. Monte Carlo simulations of luminescence processes under quasi-equilibrium (QE) conditions. *Radiation Measurements*, 67:67–76, 2014.
131. V Pagonis, J Friedrich, M Discher, A Müller-Kirschbaum, V Schlosser, S Kreutzer, R Chen, and C Schmidt. Excited state luminescence signals from a random distribution of defects: A new Monte Carlo simulation approach for feldspar. *Journal of Luminescence*, 207:266–272, 2019.
132. V Pagonis, M Jain, K J Thomsen, and A S Murray. On the shape of continuous wave infrared stimulated luminescence signals from feldspars: A case study. *Journal of Luminescence*, 153:96–103, 2014.
133. V Pagonis and G Kitis. Prevalence of first-order kinetics in thermoluminescence materials: An explanation based on multiple competition processes. *Physica Status Solidi B*, 249:1590–1601, 2012.
134. V Pagonis and G Kitis. Mathematical aspects of ground state tunneling models in luminescence materials. *Journal of Luminescence*, 168:137–144, 2015.
135. V Pagonis, G Kitis, and R Chen. A new analytical equation for the dose response of dosimetric materials, based on the Lambert W function. *Journal of Luminescence*, 225:117333, 2020.
136. V Pagonis, G Kitis, and R Chen. Superlinearity revisited: A new analytical equation for the dose response of defects in solids, using the Lambert W function. *Journal of Luminescence*, 227:117553, 2020.
137. V Pagonis, G Kitis, and C Furetta. *Numerical and practical exercises in thermoluminescence*. Springer Science & Business Media, 2006.
138. V Pagonis, G Kitis, and G S Polymeris. On the half-life of luminescence signals in dosimetric applications: A unified presentation. *Physica B: Condensed Matter*, 539:35–43, 2018.
139. V Pagonis, S Kreutzer, A R Duncan, E Rajovic, C Laag, and C Schmidt. On the stochastic uncertainties of thermally and optically stimulated luminescence signals: A Monte Carlo approach. *Journal of Luminescence*, 219:116945, 2020.
140. V Pagonis and C Kulp. Monte Carlo simulations of tunneling phenomena and nearest neighbor hopping mechanism in feldspars. *Journal of Luminescence*, 181:114–120, 2017.
141. V Pagonis, C Kulp, C Chaney, and M Tachiya. Quantum tunneling recombination in a system of randomly distributed trapped electrons and positive ions. *Journal of physics. Condensed matter : an Institute of Physics journal*, 29:365701, September 2017.
142. V Pagonis, J L Lawless, R Chen, and ML Chithambo. Analytical expressions for time-resolved optically stimulated luminescence experiments in quartz. *Journal of Luminescence*, 131(9):1827–1835, 2011.
143. V Pagonis, S M Mian, M L Chithambo, E Christensen, and C Barnold. Experimental and modelling study of pulsed optically stimulated luminescence in quartz, marble and beta irradiated salt. *Journal of Physics D: Applied Physics*, 42(5):055407, 2009.
144. V Pagonis, P Morthekai, Singhvi A K, Thomas J, Balaram V, Kitis G, and Chen R. Time-resolved infrared stimulated luminescence signals in feldspars: Analysis based on exponential and stretched exponential functions. *Journal of Luminescence*, 132(9):2330–2340, 2012.
145. V Pagonis, H Phan, D Ruth, and G Kitis. Further investigations of tunneling recombination processes in random distributions of defects. *Radiation Measurements*, 58:66–74, 2013.
146. V Pagonis, G S Polymeris, and G Kitis. On the effect of optical and isothermal treatments on luminescence signals from feldspars. *Radiation Measurements*, 82:93–101, 2015.
147. V Pagonis and P Truong. Thermoluminescence due to tunneling in nanodosimetric materials: A Monte Carlo study. *Physica B: Condensed Matter*, 531:171–179, 2018.
148. V Pagonis, A G Wintle, and R Chen. Simulations of the effect of pulse annealing on optically-stimulated luminescence of quartz. *Radiation Measurements*, 42(10):1587–1599, 2007.

149. V Pagonis, A G Wintle, R Chen, and X L Wang. A theoretical model for a new dating protocol for quartz based on thermally transferred OSL (TT-OSL). *Radiation Measurements*, 43:704–708, 2008.
150. J Peng, Z Dong, and F Han. tgcd: An R package for analyzing thermoluminescence glow curves. *SoftwareX*, 5:112–120, 2016.
151. J Peng and V Pagonis. Simulating comprehensive kinetic models for quartz luminescence using the R program KMS. *Radiation Measurements*, 86:63–70, 2016.
152. S A Petrov and I K Bailiff. Thermal quenching and the initial rise technique of trap depth evaluation. *Journal of Luminescence*, 65(6):289–291, 1996.
153. S A Petrov and I K Bailiff. Determination of trap depths associated with tl peaks in synthetic quartz (350–550 k). *Radiation Measurements*, 27(2):185–191, 1997.
154. G S Polymeris. OSL at elevated temperatures: Towards the simultaneous thermal and optical stimulation. *Radiation Physics and Chemistry*, 106:184–192, 2015.
155. G S Polymeris, V Pagonis, and G Kitis. Thermoluminescence glow curves in preheated feldspar samples: An interpretation based on random defect distributions. *Radiation Measurements*, 97:20–27, 2017.
156. G S Polymeris, V Pagonis, and G Kitis. Investigation of thermoluminescence processes during linear and isothermal heating of dosimetric materials. *Journal of Luminescence*, 222:117142, 2020.
157. G S Polymeris, N Tsirliganis, Z Loukou, and G Kitis. A comparative study of the anomalous fading effects of TL and OSL signals of durango apatite. *Physica Status Solidi (a)*, 203(3):578–590, 2006.
158. N R J Poolton, K B Ozanyan, J Wallinga, A S Murray, and L Bøtter-Jensen. Electrons in feldspar II: a consideration of the influence of conduction band-tail states on luminescence processes. *Physics and Chemistry of Minerals*, 29(3):217–225, 2002.
159. N R J Poolton, J Wallinga, A S Murray, E Bulur, and L Bøtter-Jensen. Electrons in feldspar I: on the wavefunction of electrons trapped at simple lattice defects. *Physics and Chemistry of Minerals*, 29(3):210–216, April 2002.
160. F Preusser, M Chithambo, T Götte, M Martini, K Ramseyer, E J Sendezera, G Susino, and A G Wintle. Quartz as a natural luminescence dosimeter. *Earth-Science Reviews*, 97(1):184–214, 2009.
161. J T Randall and M H F Wilkins. Phosphorescence and electron traps. I. The study of trap distributions. *Proceedings of the Royal Society of London A: Mathematical, Physical and Engineering Sciences*, 184(999):366–389, 1945.
162. M S Rasheedy. On the general-order kinetics of the thermoluminescence glow peak. *J. Phys.: Condens. Matter*, 5:633–636, 1993.
163. E Şahiner, G Kitis, V Pagonis, N Meriç, and G S Polymeris. Tunnelling recombination in conventional, post-infrared and post-infrared multi-elevated temperature IRSL signals in microcline K-feldspar. *Journal of Luminescence*, 188:514–523, 2017.
164. N Salah. Nanocrystalline materials for the dosimetry of heavy charged particles: A review. *Radiation Physics and Chemistry*, 80(1):1–10, 2011.
165. D C W Sanderson and R J Clark. Pulsed photostimulated luminescence of alkali feldspars. *Radiation Measurements*, 23(2):633–639, 1994.
166. I K Sfampa, G S Polymeris, N Tsirliganis, V Pagonis, and G Kitis. Prompt isothermal decay of thermoluminescence in an apatite exhibiting strong anomalous fading. *Nuclear Instruments and Methods in Physics Research Section B: Beam Interactions with Materials and Atoms*, 320:57–63, 2014.
167. J S Singarayer and R M Bailey. Further investigations of the quartz optically stimulated luminescence components using linear modulation. *Radiation Measurements*, 37(4):451–458, 2003.
168. J S Singarayer and R M Bailey. Component-resolved bleaching spectra of quartz optically stimulated luminescence: preliminary results and implications for dating. *Radiation Measurements*, 38:111–118, 2004.

169. L L Singh and R K Gartia. Theoretical derivation of a simplified form of the OTOR/GOT differential equation. *Radiation Measurements*, 59:160–164, 2013.
170. K Soetaert, T Petzoldt, and R Setzer. Solving differential equations in R: Package deSolve. *Journal of Statistical Software, Articles*, 33(9):1–25, 2010.
171. Karline Soetaert, Jeff Cash, and Francesca Mazzia. *Solving differential equations in R*. Springer Science & Business Media, 2012.
172. H Sun and Y Sakka. Luminescent metal nanoclusters: controlled synthesis and functional applications. *Science and Technology of Advanced Materials*, 15(1):014205, 2014.
173. C M Sunta, W E F Ayta, J F D Chubaci, and S Watanabe. A critical look at the kinetic models of thermoluminescence: I. first-order kinetics. *Journal of Physics D: Applied Physics*, 34(17):2690–2698, aug 2001.
174. C M Sunta, W E F Ayta, J F D Chubaci, and S Watanabe. A critical look at the kinetic models of thermoluminescence II. non-first order kinetics. *Journal of Physics D: Applied Physics*, 38(1):95–102, dec 2004.
175. M Tachiya and A Mozumder. Decay of trapped electrons by tunnelling to scavenger molecules in low-temperature glasses. *Chemical Physics Letters*, 28(1):87–89, 1974.
176. M Tachiya and A Mozumder. Kinetics of geminate-ion recombination by electron tunnelling. *Chemical Physics Letters*, 34(1):77–79, 1975.
177. P Thioulouse, E A Giess, and I F Chang. Investigation of thermally stimulated luminescence and its description by a tunneling model. *Journal of Applied Physics*, 53(12):9015–9020, 1982.
178. J S Thomsen. Logical relations among the principles of statistical mechanics and thermodynamics. *Phys. Rev.*, 91:1263–1266, Sep 1953.
179. A Timar-Gabor, D Constantin, J P Buylaert, M Jain, A S Murray, and A G Wintle. Fundamental investigations of natural and laboratory generated SAR dose response curves for quartz OSL in the high dose range. *Radiation Measurements*, 81:150–156, 2015.
180. A Timar-Gabor, A Vasiliniuc, D A G Vandenberghe, C Cosma, and A G Wintle. Investigations into the reliability of SAR-OSL equivalent doses obtained for quartz samples displaying dose response curves with more than one component. *Radiation Measurements*, 47(9):740–745, 2012.
181. F Trompier, C Bassinet, S Della Monaca, A Romanyukha, R Reyes, and I Clairand. Overview of physical and biophysical techniques for accident dosimetry. *Radiation protection dosimetry*, 144:571–574, March 2011.
182. S. Tsukamoto, P.M. Denby, A.S. Murray, and L. Bøetter-Jensen. Time-resolved luminescence from feldspars: New insight into fading. *Radiation Measurements*, 41(7):790–795, 2006.
183. D A G Vandenberghe, M Jain, and A S Murray. Equivalent dose determination using a quartz isothermal TL signal. *Radiation Measurements*, 44(5):439–444, 2009.
184. R Visocekas. Tunneling radiative recombination in K-feldspar sanidine. *Nuclear Tracks and Radiation Measurements*, 21:175–178, 1993.
185. R Visocekas, V Tale, A Zink, and I Tale. Trap spectroscopy and tunnelling luminescence in feldspars. *Radiation Measurements*, 29:427–434, 1998.
186. M P R Wáligorski and R Katz. Supralinearity of peak 5 and peak 6 in TLD-700. *Nuclear Instruments and Methods*, 172(3):463–470, 1980.
187. M P R Wáligorski, P Olko, P Bilski, M Budzanowski, and T Niewiadomski. Dosimetric Characteristics of LiF:Mg,Cu,P Phosphors - A Track Structure Interpretation. *Radiation Protection Dosimetry*, 47(1–4):53–58, 05 1993.
188. X L Wang, A G Wintle, and Y C Lu. Thermally transferred luminescence in fine-grained quartz from Chinese loess: Basic observations. *Radiation Measurements*, 41(6):649–658, 2006.
189. A Wieser, Y Göksu, D F Regulla, and A Waibel. Unexpected superlinear dose dependence of the E1' centre in fused silica. *International Journal of Radiation Applications and Instrumentation. Part D. Nuclear Tracks and Radiation Measurements*, 18(1):175–178, 1991.
190. A G Wintle. Thermal Quenching of Thermoluminescence in Quartz. *Geophysical Journal International*, 41(1):107–113, 1975.

191. A G Wintle and A S Murray. The relationship between quartz thermoluminescence, photo-transferred thermoluminescence, and optically stimulated luminescence. *Radiation Measurements*, 27(4):611–624, 1997.
192. A G Wintle and A S Murray. Towards the development of a preheat procedure for OSL dating of quartz. *Radiation Measurements*, 29(1):81–94, 1998.
193. X H Yang and S W S McKeever. The pre-dose effect in crystalline quartz. *Journal of Physics D: Applied Physics*, 23(2):237, 1990.
194. D Yossian and Y S Horowitz. Mixed-order and general-order kinetics applied to synthetic glow peaks and to peak 5 in LiF:Mg, Ti (TLD-100). *Radiation Measurements*, 27(3):465–471, 1997.
195. E G Yukihara and S W S McKeever. Optically stimulated luminescence. Book, 2011.
196. E G Yukihara, V H Whitley, J C Polf, D M Klein, S W S McKeever, A E Akselrod, and M S Akselrod. The effects of deep trap population on the thermoluminescence of Al_2O_3:C. *Radiation Measurements*, 37(6):627–638, 2003.
197. J Zimmerman. The radiation-induced increase of the 100 °C thermoluminescence sensitivity of fired quartz. *Journal of Physics C: Solid State Physics*, 4(18):3265–3276, 1971.